International Journal of Biological Macromolecules 263 (2024) 130188

Contents lists available at ScienceDirect

International Journal of Biological Macromolecules

journal homepage: www.elsevier.com/locate/ijbiomac

# Microbially synthesized poly(hydroxybutyrate-*co*-hydroxyhexanoate) with low to moderate hydroxyhexanoate content: Properties and applications

Isabel Thiele [a,1], Lara Santolin [a,1], Klas Meyer [b], Rainhard Machatschek [c], Uwe Bölz [d], Natalia A. Tarazona [c,*], Sebastian L. Riedel [a,e,**]

[a] Technische Universität Berlin, Institute of Biotechnology, Chair of Bioprocess Engineering, Berlin, Germany
[b] Bundesanstalt für Materialforschung und -prüfung (BAM), Berlin, Germany
[c] Institute of Active Polymers, Helmholtz-Zentrum Hereon, Teltow, Germany
[d] HPX Polymers GmbH, Tutzing, Germany
[e] Berliner Hochschule für Technik, Department VIII – Mechanical Engineering, Event Technology and Process Engineering, Environmental and Bioprocess Engineering Laboratory, Berlin, Germany

ARTICLE INFO

*Keywords:*
Bioplastic
PHA
Polyhydroxyalkanoate
Poly(hydroxybutyrate-*co*-hydroxyhexanoate)
*Ralstonia eutropha*
Biodegradable
Mechanical testing

ABSTRACT

Plastic pollution is the biggest environmental concern of our time. Breakdown products like micro- and nanoplastics inevitably enter the food chain and pose unprecedented health risks. In this scenario, bio-based and biodegradable plastic alternatives have been given a momentum aiming to bridge a transition towards a more sustainable future. Polyhydroxyalkanoates (PHAs) are one of the few thermoplastic polymers synthesized 100 % via biotechnological routes which fully biodegrade in common natural environments. Poly(hydroxybutyrate-*co*-hydroxyhexanoate) [P(HB-*co*-HHx)] is a PHA copolymer with great potential for the commodity polymers industry, as its mechanical properties can be tailored through fine-tuning of its molar HHx content. We have recently developed a strategy that enables for reliable tailoring of the monomer content of P(HB-*co*-HHx).

Nevertheless, there is often a lack of comprehensive investigation of the material properties of PHAs to evaluate whether they actually mimic the functionalities of conventional plastics. We present a detailed study of P(HB-*co*-HHx) copolymers with low to moderate hydroxyhexanoate content to understand how the HHx monomer content influences the thermal and mechanical properties and to link those to their abiotic degradation. By increasing the HHx fractions in the range of 2 – 14 mol%, we impart an extension of the processing window and application range as the melting temperature ($T_m$) and glass temperature ($T_g$) of the copolymers decrease from $T_m$ 165 °C to 126 °C, $T_g$ 4 °C to −5.9 °C, accompanied by reduced crystallinity from 54 % to 20 %. Elongation at break was increased from 5.7 % up to 703 % at 14 mol% HHx content, confirming that the range examined was sufficiently large to obtain ductile and brittle copolymers, while tensile strength was maintained throughout the studied range. Finally, accelerated abiotic degradation was shown to be slowed down with an increasing HHx fraction decreasing from 70 % to 55 % in 12 h.

## 1. Introduction

Whether it is packaging material, cutlery, clothing, household items or construction, plastic is ubiquitous, and it is hard to imagine life without it. To date, most of the 400 million tons of plastics produced yearly worldwide are derived from petroleum-based precursors, dominated by poly-olefines like poly(propylene) (PP), poly(ethylene) (PE), poly(vinyl chloride) (PVC), poly(urethanes), poly(ethylene terephthalate) (PET), and polystyrene (PS) and their copolymers with versatile properties. While efforts have been made to produce plastics deriving from renewable alternatives, the market of bio-based plastic is still small (0.5 % of total capability), even though it is steadily increasing with a current production capacity of 2.22 million tons, expected to increase to 6.30 million tons by 2027 [1]. With drop-in alternatives such

* Corresponding author.
** Correspondence to: S.L. Riedel, Berliner Hochschule für Technik, Department VIII – Mechanical Engineering, Event Technology and Process Engineering, Environmental and Bioprocess Engineering Laboratory, Berlin, Germany.
*E-mail addresses:* natalia.tarazona@hereon.de (N.A. Tarazona), riedel@tu-berlin.de, sebastian.riedel@bht-berlin.de (S.L. Riedel).
[1] These authors contributed equally to this work and share first authorship.

https://doi.org/10.1016/j.ijbiomac.2024.130188
Received 24 October 2023; Received in revised form 25 January 2024; Accepted 12 February 2024
Available online 17 February 2024

as Bio-PE, Bio-PET, and Bio-PP (bio-based and non-degradable), synthesized mostly based on sugar and starch, pollution of the environment by absence of recycling or end-of-life strategies is still a major issue due to their lack of biodegradability [2].

Polyhydroxyalkanoates (PHAs) are a well-known and much-researched group of biopolymers that are both biodegradable and can be produced from renewable raw materials, including biogenic waste streams not competing with food and feed. A variety of microorganisms are known to synthesize PHAs as intracellular carbon and energy storage compounds with a wide range of monomers and combinations thereof. The model organism of PHA metabolism is *Cupriavidus necator* (formerly known as *Ralstonia eutropha*), a Gram-negative β-proteobacterium that accumulates PHA as a carbon and energy store when stress conditions or nutrient deficiencies prevail. PHA monomers can be classified according to their side chain length into short chain length (*scl*, ≤5 carbon atoms) or medium chain length (*mcl*, ≥6 carbon atoms) [3]. Polyhydroxybutyrate (PHB), a *scl*-PHA, is best known and is naturally produced by *C. necator* wild-type. However, PHB is highly crystalline and brittle and possesses a rather narrow processing window (melting temperature of around 170 – 180 °C, which is close to the thermal decomposition temperature [4]. Compared to PP which breaks at elongation around 700 %, PHB hardly exceeds 10 %, with typical values between 1 and 3 % [5,6]. Copolymers of *scl*- and *mcl*-monomers, on the other hand, like P(HB-*co*-HHx) can reach properties comparable to PP or PE, depending on the molar content of the *mcl*-monomers, and therefore are more likely to substitute commodity plastics for certain applications [7]. *C. necator* Re2058/pCB113, which harbors a synthetic PHA operon expressing a heterologous PHA synthase capable of incorporating HB and HHx monomers into the polymer (PhaC2 from *Rodococcus aetherivorans*) and a heterologous enoyl coenzyme A (enoyl-CoA) hydratase (PhaJ from *Pseudomonas aeruginosa*) was engineered to produce the copolymer P(HB-*co*-HHx) when fed with fatty acids containing feedstocks [8]. It has been shown that the material properties of P(HB-*co*-HHx) can be tailored by controlling its HHx molar content as the incorporation of *mcl*-HA units gradually lowers its crystallinity and melting temperature while increasing ductility and toughness. This way, properties similar to low-density polyethylene can be achieved while broadening the processing window [3,7,9–12]. Although PHAs have been shown to degrade in different environments, and multiple enzymes such as lipases and depolymerases have been isolated and tested for the hydrolysis in controlled environments, these polymers are not exempt of the end-of-life (EoL) concerns. This gets aggravated as the number of copolymers of PHA increases aiming to improve their mechanical properties and thus expand their applications, requiring holistic studies to determine the structure-properties-degradability relationship of the final polymer and thus their suitable EoL management.

However, it is not clear how small variations in the copolymer's molar composition (differences between 2 and 3 % molar content) could change the degradability behavior of the final copolymer, and the gains and losses in mechanical properties versus degradability in these copolymers are not defined yet.

We have recently reported the production of tailor-made P(HB-*co*-HHx) with adjusted HHx monomer contents from 2 to 17 mol% using a simple batch strategy with defined mixtures of fructose and canola oil as substrates for *C. necator* Re2058/pCB113 [13]. In the present study we carried out a comprehensive material characterization of P(HB-*co*-HHx) with low to moderate molar HHx content to understand how their structural, thermal, and mechanical properties can be influenced, as well as how these properties affect the degradation behavior of the copolymer in accelerated conditions. For the latter the Langmuir-Blodgett method optimized for the degradation of copolymers, especially surface degradation, was used. This method has a withstanding sensibility which makes it ideal to detect minor changes in the degradation behavior of polymers [14,15], otherwise difficult to detected by studying bulk degradation processes with conventional methods such as spectroscopy, chromatography, gravimetry, microscopy, and mechanical testing. Finally, we evaluate the functionalities of the copolymers to point out suitable applications for each specific P(HB-*co*-HHx) copolymer.

## 2. Material and methods

### 2.1. Molar specific P(HB-co-HHx) production and recovery

1-L batch bioreactor cultivations using defined mixtures of fructose and canola oil with the strain *C. necator* Re2058/pCB113 for the production of tailor-made P(HB-*co*-HHx) copolymers with defined HHx contents has been described previously by Santolin, Thiele and coworkers [13].

### 2.2. Extraction of P(HB-co-HHx)

To recover P(HB-*co*-HHx) from bioreactor cultivations the complete microbial culture was harvested after 72 h, centrifuged at 4 °C and 4000 ×*g* for 30 min and the resulting biomass was dried for 72 h by lyophilization. For the extraction of the polymer, the freeze-dried cells (~10 g) were dissolved in 100 mL HPLC-grade Chloroform (VWR International GmbH, Germany) and incubated for 4 h at 50 °C in a rotary evaporator equipped with a reflux condenser (Rotavapor-RE, Büchi, Germany). The chloroform-PHA mixture was filtered through a 90-mm diameter glass microfiber filter (Whatman, Global Life Sciences Solutions, USA) and the PHA was precipitated in 250-mL PTFE centrifugation bottles (FEP Nalgene, Thermo Fisher Scientific Inc., USA) by slowly pouring 50 mL of the solution into 200 mL ice-cold HPLC-grade methanol (VWR International GmbH, Germany). The bottle was filled up to 100 % with methanol and centrifuged for 20 min at 4 °C and 4000 ×*g*. After centrifugation, the supernatant was discarded and the PHA pellet was washed twice by filling the bottle again with methanol, mixing and centrifuging. The extracted PHA was streaked on a glass petri dish and left to dry for 3 d in the fume cupboard.

### 2.3. Determination of molecular weight characteristics

Molecular weight was determined by gel permeation chromatography (GPC) equipped with a differential refractive index detector (Merck-Hitachi, RI-Detector L-7490) using two sequentially coupled columns (Agilent PLgel 5 μm MIXED-C300 × 7.5 mm, 50 × 7.5 mm Guard). Polystyrene standards in the range of 9.6–3187 kDa were used for calibration (Agilent Polystyrol PS-1). PHA samples were weighed to obtain a concentration of 5 mg $mL^{-1}$ in 2 mL of chloroform containing 2-butanone at a concentration of 1 mg $mL^{-1}$ in a borosilicate tube (Borosilicate Screw Thread Culture Tube with PTFE-Faced Rubber Lined Caps, Ø16 mm x 100 mm, KIMAX) and incubated at 55 °C for 24 h (Hettich Lab Technology). After cooling to room temperature, the samples were filtered into an amber HPLC vial through 0.2 μm PTFE syringe filters. Analysis of 15 μL samples was performed at 30 °C and a flow rate of 0.8 mL $min^{-1}$ chloroform. Molecular weights, calculated by the calibration data were used to calculate the number average (Mn), weight average (Mw), and dispersity values (Đ) according to equations described previously [16].

### 2.4. NMR analyses

$^{1}H$ and $^{13}C$ NMR studies were performed on a 500 MHz NMR spectrometer system (VNMRS500, Varian Associates, USA) equipped with a OneNMR probe for standard 5 mm NMR tubes. About 10 mg of each sample were dissolved in 0.6 mL $CDCl_3$ and studied at room temperature. $^{1}H$ NMR spectra were acquired as single scans, while for $^{13}C$ NMR spectra in total 4096 scans were accumulated.

Signals in the $^{1}H$ NMR spectrum were assigned to the monomers HB and HHx according to literature [16]. HHx content ($F_{HHx}$ – Fraction of HHx) was determined by relative quantification based on Eq. (1) by

using integrated signals ($I_{HHx}$ and $I_{HB}$) of HHx at 1.56 ppm and HB at 1.26 ppm. The latter showed an overlap with the $CH_2$-signal of HHx, which was compensated by subtracting the signal area by the amount of $CH_2$-signal at 1.56 ppm.

$$F_{HHx} = \frac{I_{HHx}}{I_{HHx} + I_{HB}} \quad (1)$$

Randomness (D) of the copolymer was estimated by the ratio of signal areas of quaternary carbons of C═O functional groups within the $^{13}C$ NMR spectra in the range from 169.1 to 169.5 ppm (see Eq. (2)) [16].

$$D = \frac{F_{HB-HB} \times F_{HHx-HHx}}{F_{HB-HHx} \times F_{HHx-HB}} \quad (2)$$

### 2.5. Differential Scanning Calorimetry (DSC)

The thermal properties of the copolymers were analyzed by DSC (DSC 204 F1, NETZSCH, Germany). About 5 mg samples of the copolymers were heated and cooled at a rate of 10 K $min^{-1}$ from −50 to 200 °C in aluminum pans under inert nitrogen (1 K $min^{-1}$ in the case of P(HB-*co*-14.3 mol%HHx). $T_g$ and $T_c$ were determined from the second heating. A melting enthalpy of 146 J $g^{-1}$ (theoretical value of 100 % crystalline P(3HB) [17]) was used to extrapolate the sample crystallinity. The Netzsch Proteus software was used to extract the transition temperatures and enthalpies from the experimental data.

### 2.6. Mechanical testing

Copolymer specimens were produced by solvent evaporation of copolymer/chloroform solutions. Films with a thickness between 0.5 and 0.9 mm, a width of 2 mm, and a length of 15 mm were cut with a dogbone shape and utilized for mechanical testing. Before testing, the test-specimens were incubated at their crystallization temperature overnight to accelerate the crystallization process so that mechanical properties representing those after physical ageing were obtained. Tensile testing was carried out at ambient temperature with a Zwick Z005 (Zwick GmbH, Germany). The stretching rate was kept constant at 10 mm $min^{-1}$ for all tensile tests. At least two samples were investigated for each copolymer. The stress vs. strain curves are available in the supplementary materials Fig. S7. The Young's modulus (E) was determined from the stress–strain curve in the strain region of 1–5 %

### 2.7. Characterization of P(HB-co-HHx) surface behavior in aqueous environments

To study the behavior of P(HB-*co*-HHx) on aqueous environments, latter needed for degradation studies, copolymer films were prepared using the Langmuir-Blodgett (LB) method. LB films are 2D organized thin films "floating" on a liquid surface (e.g., Phosphate-buffered saline, PBS), prepared by depositing a known concentration of copolymer molecules in chloroform on a well-defined volume of PBS, which is contained in a Langmuir trough made of polytetrafluoroethylene. Thus, LB films mimic the surface of a material and the plasticizing effect of water on its surface. The trough used for the characterization of the P(HB-*co*-HHx) 2D films has an area of 243 $cm^2$ (KSV NIMA, Finland) and it is connected to a surface tensiometer (Wilhelmy plate microbalance) that measures the changes in the surface tension of the water (surface pressure $\pi$) upon the formation of 2D films on the air-water interface. The trough is equipped with two movable barriers that allow for precise control of the mean molecular area (MMA); area occupied per repeating unit of the copolymer at the air-water interface. The changes in $\pi$ upon compression of the molecules on the surface at a constant temperature are recorded as $\pi$-MMA isotherms.

To obtain π-MMA isotherms, P(HB-*co*-HHx) solutions were prepared in chloroform at a typical concentration of 0.15 mg $mL^{-1}$. 60 μL of the chloroform solution were spread dropwise at the air-water interface using 170 mL PBS as the liquid subphase. Thus, about 8.5 μg of polymer were applied in each experiment. Before compression of the monolayer, the chloroform was allowed to evaporate for 10 min to avoid interference in the π measurement. The Langmuir layers were laterally compressed with the barriers at constant compression rates of 10 mm $min^{-1}$. The MMA for the P(HB-*co*-HHx) films was calculated based on the mass of the film and on the average mass of a repeating unit, based on the HB and HHx content, and the surface area of the trough during compression. An example calculation is shown in the supplemental material (Eq. (S1)). All isotherms were recorded at 21 °C ± 0.5. Compression isotherms are reproducible with a random measurement error of ≈5 % concerning the surface pressure or the MMA values for the independently repeated experiments.

### 2.8. Langmuir monolayer degradation (LMD) experiments

#### 2.8.1. pH 12.3

Degradation experiments were carried out using the medium size Langmuir trough with the setup explained above. Hydrolytic degradation of P(HB-*co*-HHx) films was tested in subphases consisting of aqueous KOH solutions with pH = 12.3, which was demonstrated to be the lowest pH (in the basic scale) at which PHB is hydrolysable within hours in a 2D system [15]. Initially, the layers were compressed and held at $\pi_D$ = 10 mN $m^{-1}$ on a MilliQ water subphase (pH = 6). After around 20 min, the pH of the subphase was adjusted to pH = 12.3 by addition of 5 mL 10 M KOH (Merck, ultrapure) under the films (into the water subphase). The pH of the subphase was monitored at given points of the experiment, and a water compensation tool was used for long-term degradation experiments. The loss of small water-soluble fragments from the interface, generated during hydrolysis of the copolymer chains, was compensated by the lateral compression of the barriers to maintain constant surface pressure $\pi_D$. Area loss is expressed as $A\,A_0^{-1}$ in %, where A corresponds to the area of the film at time t and $A_0$ corresponds to the initial MMA where the KOH solution was injected, which corresponds to $\pi_D$ = 10 mN $m^{-1}$ in all cases.

#### 2.8.2. pH 1.2

The acid-catalyzed hydrolysis of ester bonds has been described for polyesters such as poly(ε-caprolactone) in a 2D system at 20 °C in the pH range of 2.5 and 1.2. Hydrolytic degradation of P(HB-*co*-HHx) films was tested in subphases consisting of aqueous HCl solutions with a final pH = 1.2. Initially, the layers were compressed and held at $\pi_D$ = 10 mN $m^{-1}$ on a MilliQ water subphase (pH = 6). After stabilization of the surface pressure for around 50 min, the pH of the subphase was adjusted to pH = 1.2 by the addition of 0.42 mL of a 12 M HCl solution per 100 mL of subphase under the films to obtain a 0.05 M HCl solution under the films. The pH of the subphase was monitored at given points of the experiment. The loss of small water-soluble fragments from the interface, generated during hydrolysis of the copolymer chains, was compensated by the lateral compression of the barriers to maintain constant surface pressure $\pi_D$. Area loss is calculated by the difference in film area (MMA) at a surface pressure of 10 mN $m^{-1}$ before and after degradation.

## 3. Results and discussion

### 3.1. Determination of randomness of P(HB-co-HHx) as a function of the HHx content

$^1H$ and $^{13}C$ NMR spectra of the six P(HB-*co*-HHx) copolymers used in this study were analyzed and used to determine the molar HHx fraction and degree of randomness (Tables 1, S1). The determination of the molar fraction of HHx in the copolymers determined from the $^1H$ NMR spectra were in close agreement with the data acquired by GC measurements (Table 1, Fig. S1).

**Table 1**
Analysis of the molar composition of P(HB-*co*-HHx) and randomness (D) determination of molar specific P(HB-*co*-HHx) samples by $^{1}$H and $^{13}$C-Nuclear Magnetic Resonance studies.

| HHx [mol%] (GC)[a] | HHx [mol%] (NMR) | Randomness D [−] |
|---|---|---|
| 2.3 | 2.66 | – |
| 4.3 | 4.56 | 8.01 |
| 6.5 | 6.81 | 5.49 |
| 7.5 | 7.93 | 4.83 |
| 11.4 | 10.56 | 2.80 |
| 14.3 | 14.20 | 1.79 |

HHx molar content of P(HB-*co*-HHx) (HHx, mol%) and Randomness calculation (D) determined by $^{1}$H NMR (single scans) and $^{13}$C NMR (4096 scans) is shown.
[a] From Santolin et al. [13].

The degree of randomness (*D*) of the copolymers was calculated from $^{13}$C NMR spectra (Table 1, Fig. S2). The statistical sequence distribution was determined based on the ratio of the resonances' areas, corresponding to the dyads of HB and HHx monomers, the statistical sequence distribution was determined. For *D* values close to 1 ($D \approx 1$) a randomness can be assumed, while $D \gg 1$ indicate block organization and $D < 1$ alternating arrangement of HB and HHx units [16]. Our study shows that all copolymers had a D value above 1 with increasing blocky nature of the copolymer up to a D value of 8 when only fractions of HHx as low as 4.3 mol% were present. The copolymer containing 2.3 mol% HHx shows no meaningful data regarding randomness, due to the low content of HHx and therefore too low signal to noise ratio (SNR) within the $^{13}$C NMR spectrum. The blocky nature of all samples described by NMR is a consequence of the overall low range of HHx contents studied as the high excess of HB monomers forces the formation of blocks. Moreover, due to the increased incorporation of HHx precursors at the beginning of the cultivations it is likely that the copolymer has some blocky structure NMR as a consequence of the enzymatic activity of PHA synthase that controls the polymerization of both HB-coenzyme A (HB-CoA) and HHx-CoA monomers into the copolymer chain inside the bacterial cytoplasm [18,19]. If the availability of HB monomers is higher for HB, the monomers would get preferentially polymerized into a block. When the differences in the content of HB and HHx monomers are less evident, the randomization could occur due to the affinity of the PHA synthase (recombinant PhaC2 from *R. aetherivorans*) for both HB-CoA and HHx-CoA.

In agreement with Purama et al. [12] who obtained D values close to 1 for P(HB-*co*-HHx) with HHx fractions from 12 to 28 mol%, the P(HB-*co*-HHx) copolymer with the highest HHx content in this study (14.3 mol % HHx), with a D value of 1.79, shows a distribution closest to random, indicating an overall random distribution of HHx monomers within the copolymer. In general, there is no agreement in literature on the value at which a copolymer is no longer considered to have a random distribution but a block structure, even though PHA copolymers are generally classified as random. While some studies regard PHA copolymers with high HHx contents >50 mol% with D values of 1.37–2.35 as "not random" [20], different studies categorize PHA copolymers with a D value of 2.29 still as random when the copolymer contained 17.3 mol% HHx [16]. Nonetheless it is important to remark that NMR analysis remains limited and information like sequence distribution, clusters, or gradients cannot be exactly provided by NMR spectroscopy [21].

### 3.2. Thermal properties of P(HB-co-HHx) with increasing HHx molar content

DSC analysis was performed to characterize the thermal properties of the copolymers. A first heating cycle was performed to remove the thermal history of previous processing of the copolymers. With increasing HHx content, the glass transition temperature ($T_g$) shifted down from 4 °C to −5.9 °C when the molar HHx content increased from 2.3 to 14.3 HHx mol% (Table 2, Fig. S3). For PHA polymers, the $T_g$ is generally lower when longer side chain monomers are integrated into the polymer indicating an enhanced segmental mobility of the polymer chains [22]. Endothermic peaks between 165 °C and 126 °C (for the first heating cycle) and between 162 °C and 121 °C (for the second heating cycle) denoted the melting temperature ($T_m$), shifting to lower temperatures with increasing HHx content. The observed trends are in high agreement with literature values that report decreasing melting temperatures with the incorporation of HHx monomers [8,11,23,24].

Endothermic peaks between 165 °C and 126 °C (for the first heating cycle) and between 162 °C and 121 °C (for the second heating cycle) denoted the melting temperature and became smaller with increasing HHx content and shifted to lower temperatures. All copolymers showed several smaller melting peaks indicating recrystallization, with P(HB-*co*-14.3mol%HHx) showing the most pronounced recrystallization (see Supplementary Material S3). Murugan et al. [11] observed a melting temperature of 156 °C and a glass transition temperature of −12 °C for P(HB-*co*-15mol%HHx) and Purama et al. [12] reported a $T_m$ of 136.03 °C and a $T_g$ of −1.15 °C for P(HB-*co*-12mol%HHx). By lowering the $T_m$, a much broader processing window is achieved and thermal decomposition during processing can be avoided. During the second heating cycle of P(HB-*co*-14.3mol%HHx), two melting peaks at 121 °C and 131 °C (at 1 K min$^{-1}$) were observed which can either be attributed to recrystallization events or to a blocky copolymer distribution [25] that would contradict the NMR data showing the most random distribution for this copolymer. The multiple melting behavior of P(HB-*co*-HHx) is actually common in PHAs and was thoroughly analyzed by Hu et al. [26] using DSC and FT-IR (Fourier transform infrared spectroscopy) measurements. This phenomenon was assigned to the fact that the bulky side group the long-range packing gets disrupted and leads to decreased crystallinity and reduced crystallization rates, becoming evident as multiple and shifted melting peaks by the melt-recrystallization-remelting process during heating. As HHx units cannot crystallize, they disrupt the PHB crystal lattice. It is well-known that the multiple melting behavior is dependent on the heating rate which is also visible in our data.

**Table 2**
Determination of thermal properties of P(HB-*co*-HHx) copolymers depending on the molar HHx content by Differential Scanning Calorimetry.

| HHx | $T_g$ | $T_{m1}$ | $T_{m2}$ | $T_c$ | $\Delta H_{m1}$ | $\Delta H_{m2}$ | $cryst_1$ | $cryst_2$ | Crystallization during cooling |
|---|---|---|---|---|---|---|---|---|---|
| mol% | °C | °C | °C | °C | J g$^{-1}$ | J g$^{-1}$ | % | % | |
| 2.3 | 4 | 165 | 162 | 53 | 79 | 72.3 | 54 | 50 | Yes |
| 4.3 | 3.6 | 162 | 162 | 59.5 | 72.3 | 73.3 | 49 | 50 | Yes |
| 6.5 | 2.5 | 158 | 156 | 65 | 62.6 | 57.5 | 43 | 39 | No |
| 7.5 | 3 | 157 | 156 | 67 | 60.85 | 57.1 | 41 | 39 | No |
| 11.4 | 2.9 | 147 | 148 | 80 | 50.3 | 43.3 | 34 | 30 | No |
| 14.3 | −5.9 | 126 | 121, 131 | 55[a] | 29.5 | 29.5 | 20 | 20 | No |

HHx molar content of P(HB-*co*-HHx) (HHx, mol%), glass transition temperature ($T_g$, °C), melting temperature during the first heating cycle ($T_{m1}$, °C), melting temperature during the second heating cycle ($T_{m2}$,°C), crystallization temperature ($T_c$, °C), melting enthalpy during the first heating cycle ($dH_{m1}$, J g$^{-1}$), melting enthalpy during the second heating cycle ($dH_{m2}$, J g$^{-1}$), crystallinity of the sample calculated from the first melting enthalpy ($cryst_1$, %), crystallinity of the sample calculated from the second melting enthalpy ($cryst_2$, %) and crystallization during cooling is indicated.
[a] Sample was heated at 10 times lower rate, therefore cold crystallization temperature was lower.

Comparing the impact of incorporation of HHx monomers determined in this study vs. HV monomers reported in literature, we can confirm that the incorporation of HHx monomers has a higher impact on the reduction of the $T_m$ than incorporation of HV monomers [7]. The slightly lower than expected $T_g$ recorded for P(HB-*co*-6.5mol%HHx), that does not fit the overall trend, may be attributed to the reduced molecular weight of this sample ($3.2 \times 10^5$ Da) in comparison to all other samples (average $3.6 \times 10^5$ Da) (see Supplementary Table S2, Fig. S4). As described in literature, high molecular weight polymers with longer chains tend to entangle with each other more extensively. This increased entanglement can restrict molecular mobility and result in a higher $T_g$ [27].

The cold crystallization temperature, observed during the second heating, increased from 53 °C to 80 °C with increasing HHx contents from 2.3 to 11.4 mol% due to the slower crystallization rates with increasing HHX contents. Consequently, no crystallization upon heating was observed for the copolymer with the highest HHx content P(HB-*co*-14.3mol%HHx) at a heating rate of 10 K $min^{-1}$. At a lower heating rate of 1 K $min^{-1}$, P(HB-*co*-14.3mol%HHx) crystallized at a $T_c$ of 55 °C, only 2 °C higher than for the lowest HHx content tested. At the applied cooling rates, only copolymers with low HHx fractions below 6.5 mol% were able to crystallize during cooling while the copolymers with higher HHx content were not. Overall, the presence of the *mcl* fraction led to a significantly lower melting enthalpy since crystallinity decreased from 50 to 20 % for P(HB-*co*-2.3mol%HHx) and P(HB-*co*-14.3mol%HHx), respectively (Fig. 1, Table 2, Fig. S3) fitting well with the crystallinity calculated by Noda et al., which decreased from 53 % in P(HB-*co*-3mol% HHx) to 39 % for P(HB-*co*-12mol%HHx). Moreover, this further highlights the superior properties over P(HB-*co*-HV) as only a small amount of the *mcl*-monomer in P(HB-*co*-HHx) leads to a more ductile and less brittle polymer comparable to the flexible and ductile polyethylene [7], while P(HB-*co*-HV) maintains a high degree of crystallinity even at 25 mol% HV due to isodimorphism [28].

### 3.3. Mechanical testing

Prior to the characterization of material properties of the copolymers, the molecular weight was tested (Table S2, Fig. S4). If molecular weight of a linear polymer is higher, the polymer chains' entanglement might increase and thereby also increase the mechanical properties. The molecular weight of the copolymers was determined to be in a rather narrow range of $3.2–4.0 \times 10^5$ Da and is therefore assumed to not have a significant impact on the overall trend of mechanical properties and degradation. Thus, we can assign changes on these properties mainly to the molar HHx fraction.

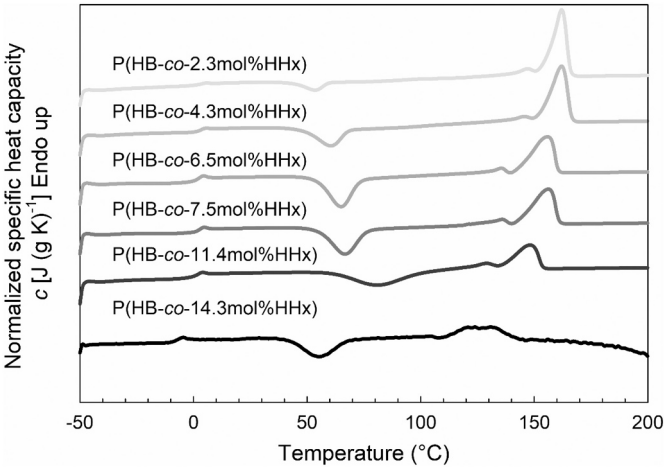


**Fig. 1.** DSC analysis of P(HB-*co*-HHx) samples with increasing HHx molar content. Second heating cycle is shown for P(HB-*co*-2.3mol%HHx), P(HB-*co*-4.3mol%HHx), P(HB-*co*-6.5mol%HHx), P(HB-*co*-7.5mol%HHx), P(HB-*co*-11.4mol%HHx) and P(HB-*co*-14.3mol%HHx). Endothermic events are displayed as upward peaks. All samples were heated at 10 K $min^{-1}$ except P(HB-*co*-14.3mol%HHx) which was heated at 1 K $min^{-1}$.

Mechanical testing showed increasing elasticity of the copolymers containing higher HHx contents. The elongation at break of P(HB-*co*-2.3mol%HHx) to P(HB-*co*-7.5mol%HHx) increased steadily from 5.7 to 40 % (Table 3). Comparing the gain in elongation at break by increasing the HHx monomer fraction, this increase is in agreement with Asrar et al. [29] reporting an increase in elongation at break from 6.7 % to 43 % for P(HB-*co*-2.5mol%HHx) to P(HB-*co*-9.5mol%HHx). Furthermore, a much more drastic change in elongation at break in the copolymers P(HB-*co*-11.4mol%HHx) and P(HB-*co*-14.3mol% HHx) was observed in this work, going from 200 % to a striking increase of up to 703 %. Moreover, P(HB-*co*-14.3mol%HHx) showed a drastic reduction of its stiffness, expressed by a Young's modulus of about 195 MPa compared to the other test specimen with a Young's modulus of 310–440 MPa. Other authors observed decreasing Young's modulus with increasing HHx monomer contents already below P(HB-*co*-11.4mol%HHx) which could not be observed for our samples [29]. In order to better understand this behavior, X-ray diffraction could be implemented in future to investigate the crystalline structure of the produced copolymers more accurately. Further studies evaluated the effect of the introduction of 32–70 mol% HHx, which led to low tensile strength and a decreasing Young's modulus to even less than 1 MPa, while delivering high values for elongation at break up to 1075 % [20].

The samples with intermediate HHx content between 6.5 and 11.4 mol% exhibited strain-induced crystallization, which was made apparent by increased opaqueness in the elongated part of the test specimen (Fig. S5). Interestingly, all samples presented fairly constant tensile strength values around 20 MPa. This effect is technically very relevant compared to petrochemical plastics that show a loss of mechanical strength parallel to the increase in toughness and elasticity when flexible olefinic monomers contents are increased in a polar polymer chain (e.g., PET, PA and TPU). Typically, a higher amount of non-polar monomers reduces the overall crystallinity and causes a lower polar intermolecular interaction that leads to a lower tensile strength in parallel to the loss in *E*-Modulus (Youngs' modulus) and the increase in elongation values. Although fairly constant, an overall downward trend in tensile strength from 22.8 to 17.5 MPa is observed especially from P(HB-*co*-4.3mol%HHx) to P(HB-*co*-11.4mol%HHx) which is in accordance to literature [29]. On the other hand, a higher degree of entanglement of the non-polar, branched HHx side chains may also increase tensile strength in elongation mode which could explain the compensation in tensile strength observed for P(HB-*co*-14.3mol%HHx).

Assessing our data, it is remarkable that the loss of stiffness at higher contents of HHx (> 10 mol%) due to lower crystallinity is not only leading to the expected higher elasticity and elongation at break, but at the same time, the increasing number of entanglements via HHx side chains seems to be completely compensating the lower crystallinity resulting in almost constant tensile strength for all tested PHA-copolymers in this study [30].

**Table 3**
Mechanical properties determined by tensile testing of P(HB-*co*-HHx) copolymers with increasing molar HHx content (average of 2–4 samples, Fig. S6).

| HHx [mol %] | Young's Modulus [MPa] | Tensile strength [MPa] | Elongation at break [%] |
|---|---|---|---|
| 2.3 | 384.4 ± 17.5 | 20.9 ± 2.3 | 5.7 ± 0.4 |
| 4.3 | 430.0 ± 32.3 | 22.8 ± 0.6 | 11.1 ± 3.8 |
| 6.5 | 321.1 ± 144.3 | 21.2 ± 2.9 | 26.2 ± 3.4 |
| 7.5 | 443.0 ± 12.6 | 20.0 ± 0.5 | 40.6 ± 6.1 |
| 11.4 | 310.4 ± 18.1 | 17.5 ± 0.94 | 200.4 ± 50.7 |
| 14.3 | 194.8 ± 16.3 | 20.2 ± 0.8 | 703.0 ± 32.3 |

HHx molar content of P(HB-co-HHx) (HHx, mol%), Young's modulus (MPa), tensile strength (MPa) and elongation at break (%) is shown.

### 3.4. Surface pressure vs. mean molecular area (π-MMA) isotherms

To enable a fast assessment of the influence of small variations in the HHx content on the degradability of the tested copolymers, LB method or LB monolayer degradation technique was used. With this set up, the copolymers are deposited as ultrathin films at the air-water interface forming a water floating 2D film. To determine the characteristics of the thin film on the water (PBS) surface and the optimal surface pressure for the degradation experiments ($\pi_D$), compression isotherms were performed by reducing the area of the available water surface by means of closing the mobile barriers. The evolution of the π is then measured as the 2D film is compressed. The π vs. MMA isotherms of three different copolymers of P(HB-*co*-HHx) were recorded at neutral pH and 21 °C on PBS (Fig. 2A). The isotherm of P(HB-*co*-2.3mol%HHx) showed a distinct kink (inset) at π of 16.6 mN $m^{-1}$ and an MMA of 13.3 $Å^2$, almost identical to the isotherm of PHB homopolymer previously reported, which suggests a phase transition accompanied by crystallization [15]. As for P(HB-*co*-6.5mol%HHx), the kink was less marked and appeared at smaller MMA of 12.5 $Å^2$, depicting the effect of HHx monomers on increasing the energy needed for compression-induced crystallization. In both cases, the surface pressure kept increasing upon compression, contrary to what was observed for P(HB-*co*-14.3mol%HHx). In the latter, the surface pressure remained constant despite compression of the layer, indicating a transition from a 2D to a 3D layer, where further compression causes the molecules to desorb and form loop like structures that surpass the A-W interface seen as a plateau in the isotherm. As suggested by DSC, P(HB-*co*-14.3mol%HHx) is crystallizing slowly at best, so the 2D-3D transition is not associated to a crystallization process. These findings correlate well to another PHA with longer side chains, poly(hydroxyoctanoate-*co*-hydroxyhexanoate) [P(HO-*co*-HHx)] with 6 mol% HHx, where a similar isotherm was observed and crystallization was ruled out by polarization-modulation infrared reflection-absorption spectroscopy (PM-IRRAS) and interfacial rheology measurements [15] as well as for isotherms referenced for poly(3-*R*-hydroxyundecenoate) (PHUE) [31]. As demonstrated by these experiments, the distinct properties of P(HB-*co*-HHx) copolymers with different HHx content determined by thermomechanical data, are also evident by the LB technique.

### 3.5. Langmuir monolayer degradation (LMD) experiments

The degradation experiments were performed at constant surface pressure $\pi_D = 10$ mN $m^{-1}$, below the phase transitions detected in the isotherms of all three copolymers, ruling out the effect of crystallinity in the degradation behavior of the films. This allowed comparing solely the impact of the molar content of the longer side-chain monomers (HHx) on the hydrolysis of P(HB-*co*-HHx). As the copolymers get hydrolyzed, oligomers and monomers are released as soluble fragments which migrate from the air-water interface to the bulk water or PBS, causing a reduction in the surface pressure. To maintain a constant surface pressure of $\pi_D = 10$ mN $m^{-1}$, the barriers are allowed to close, which is recorded as area reduction due to degradation of the polymer chains. The key advantages of this technique are the precise quantification of the mass loss via the area between the barriers, and the faster degradation when compared to bulk test specimen. The acceleration arises from the direct contact between water and monolayer, whereas bulk polymers typically take up only about 1 % of water. For conditions where polymers would undergo surface erosion, e.g. enzymatic catalysis and strongly alkaline media, the acceleration arises from the ultralow thickness. An extrapolation to the Langmuir monolayer degradation rate to bulk materials can give reasonable results when these accelerating factors are considered, but the technique is more suited for rapid assessment of the susceptibility of molecules to different catalysts and reagents, as well as the influence of molecular parameters such as architecture and crystallinity.

At pH 12.3 (Fig. 2B), the hydrolysis rate of the copolymers was reduced by the increase in the molar content of HHx. At this pH, for all samples, a fast initial degradation rate was observed, where 40–60 % of the film area was reduced. Residual hydrolysis proceeded at lower rate, which is ascribed to a slow decrease in pH due to dissolution of carbon dioxide from the ambient air. This leads to the formation of a carbonate buffered system with a typical pH of 10 after 20 h. The lower hydrolysis shown by the copolymers with higher content of HHx mol% can be ascribed to two effects: Firstly, the long side chain poses a steric hindrance for the nucleophilic attack of water or hydroxyl ions at the ester groups. Secondly, the increased randomness of P(HB-*co*-14.3mol%HHx) could influence the solubility limit of the oligomers since the solubility of HHx is lower than the solubility limit of HB. This means that chains with higher HHx content must be cut more often to generate soluble fragments. Therefore, the relative degradation velocity decreased with increasing HHx content at pH 12.3.

Under acidic conditions at pH 1.2 ± 0.2, the degradation of all PHB copolymers was negligible for about 80 h (Fig. S7), except for P(HB-*co*-2.3mol%HHx) in which 15 % area reduction was observed after 24 h. The greater degradability of polyesters under alkaline conditions when compared to acidic catalysis is already well established, also for PHB

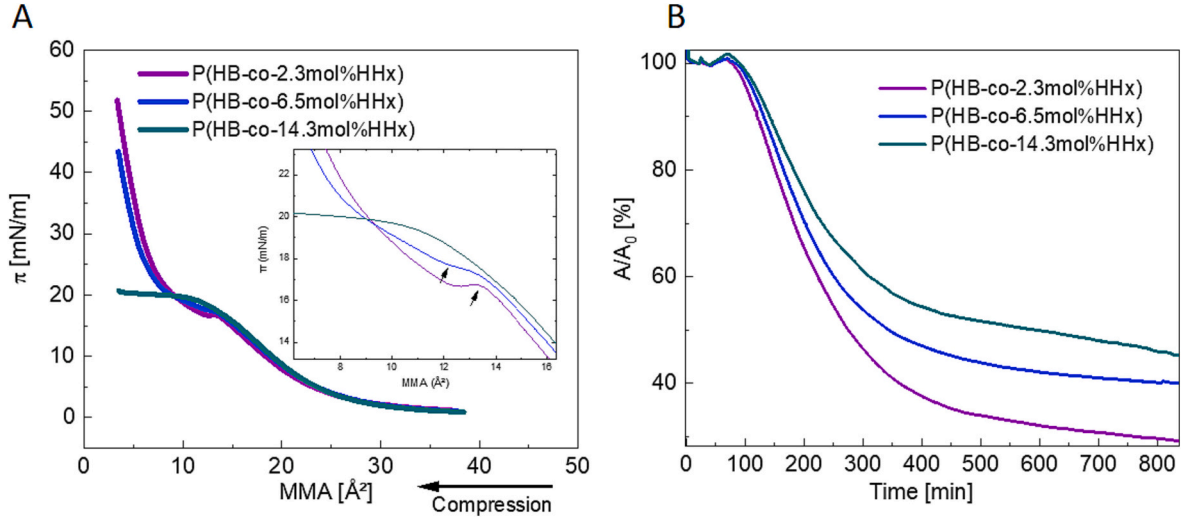


**Fig. 2.** Compression isotherms of P(HB-*co*-HHx) films with 2.3, 6.5 and 14.3 mol% HHx. All presented isotherm data correspond to individual experiments (A). Langmuir monolayer degradation at pH 12.3 (B).

[32], and here, the tendency of the HHx groups to reduce the degradability even further follows the same trend for both acidic and alkaline conditions.

Comparing our results with other studies, we find that the decreased hydrolysis rate of PHA copolymers incorporating monomers with longer side chains is also observed in bulk and at neutral pH biodegradability studies of bulk materials in soil [33,34] document an overall improved degradation of PHB when it is produced as a copolymer with longer side-chain monomers, as it results in reduced crystallinity of the bulk. As for the enzymatic-mediated degradation, some controversy is still served, since the lower crystallinity have shown benefits for enzymatic hydrolysis [35], but the longer side chains of *mcl*-monomers have been shown to add steric hindrance on the enzyme activity, decreasing the degradation rate of the copolymers. Nonetheless, although most PHA (co) polymers are efficiently degraded in the open environment, at high pH or under controlled enzymatic hydrolysis, it is important to remark that the sustainable design of PHA copolymers must be accompanied by a systematic test where minimal differences in the monomeric composition could be detected and accounted for in the degradation profiling and thus in the EoL management of the final PHA-based products.

## 4. Application perspectives

During the past decades, numerous companies producing a variety of PHA copolymers from renewable feedstocks and waste streams with a total capacity of up to 48 k tons annually were founded [36]. Opportunities for various applications arise from different monomeric compositions, especially of P(HB-*co*-HHx).

Overall, the melting range demonstrated for the P(HB-*co*-HHx) copolymers aligns closely with PP- ($T_m$ 130–165 °C, processing temperature: 150–230 °C) or PET-copolymers ($T_m$ 170–250 °C, processing temperature: 200–300 °C). Furthermore, most processing techniques are applicable, as, according to literature, the decomposition temperature of the P(HB-*co*-HHx) copolymers studied herein should be above 230 °C. Asrar et al. [29] determined the decomposition temperature of P(HB-*co*-2.5mol%HHx) with a Mw of $2.3 \times 10^5$ Da, similar to the one analyzed in this study, at 230 °C using TGA while shifting to higher temperatures with increasing HHx fraction. These comparable thermal properties, make P(HB-*co*-HHx) copolymers promising bio-based and biodegradable substitutes for products currently made from PP, PET, and PS-copolymers including applications in high performance packaging, the automotive industry, consumer goods and technical applications.

In this study, P(HB-*co*-HHx) copolymers with HHx fractions higher than 6.5 mol% exhibited low crystallinity combined with slow crystallization speed and the lowest $T_g$ values. This combination allows the production of transparent products like films, sheets (including additional thermoforming steps for containers or covers for mobile and stationary electronics) and injection molded parts [37,38]. Notably, these copolymers exhibit properties comparable to PET/PS-blends that preserve a high stiffness and optical surface quality, sufficient toughness and elasticity at room temperature, while remaining resistant to low temperatures without compromising transparency or facing embrittlement.

Also, with increasing HHx fractions, the copolymers showed reduced crystallinity, estimated by DSC, combined with an increase in tensile elongation. This combination is expected to increase impact resistance, which was already demonstrated for P(HB-*co*-HV) with increasing HV fraction [39]. To verify this, impact resistance of the copolymers could be tested by Izod or Charpy impact test [40,41]. By increasing the HHx fractions above the studied range, drastically reduced crystallinity results on completely amorphous P(HB-*co*-HHx) copolymers [20], which can be used as pressure-sensitive adhesive (PSA) coatings on P(HB-*co*-HHx) films.

Companies like Danimer Scientific, Kaneka or Bluepha are already offering a range of products made from P(HB-*co*-HHx), like bottles, recyclable paper, cutlery and straws, (cosmetics-) packaging, shopping bags, coatings, 3D printing inks or films [42]. With glass transition temperatures far below room temperature, it is known that these materials undergo time-dependent changes in material properties upon storage known as ageing [43]. This is why short-shelf-life (days, weeks, or months) packaging applications are ideal for PHAs. However, PHAs can also be applied in long shelf-life uses such as in personal care packaging as they keep their integrity and functionality just like fossil plastic containers [44].

However, completely replacing these “standard” products with biopolymers while retaining all their well-known properties and processing behavior, flexibility and stability will require significant additional effort for adapting process machinery, incorporating suitable additives, and modifying process conditions.

Regarding end-of life strategies, while standard polyesters like PET are commonly chemically recycled, bio-polyesters, especially PHAs, can as well be easily chemically modified [45] or chemically and naturally disintegrated and recycled [46].

Although holding great potential, the PHA market price is approximately 5 € $kg^{-1}$ which is about 5 times higher than conventional plastics [47]. The main cost driving factors of PHA production hindering competitiveness are represented by the substrate and extraction costs. To address this, approaches using cheap waste streams as substrates in fed-batch processes to increase production yields and achieve circular bioeconomy can be used [48]. Moreover, green downstream alternatives without halogenated solvents or even non-sterile processes using seawater have been introduced lately [49].

## 5. Conclusion and outlook

Although there is a considerable amount of data in the literature on thermal and mechanical properties, as well as their molecular weight dependence, of P(HB-*co*-HHx) copolymers with almost any monomer fraction from 1 to 70 mol% HHx [42], only a few studies are comprehensive and provide true comparability between copolymers (such as: [29]; or [20]), as otherwise differences in molecular weight are not considered or generally the variety of copolymers tested was too small.

To address this gap, we provide a detailed, comprehensive study of the impact of the molar HHx fraction of P(HB-*co*-HHx) in the range of 2–14 mol% with similar molecular weights of $3.2–4.0 \times 10^5$ Da [13] on material properties, degradability and the possible applications arising from the thermomechanical characteristics of the individual copolymers. Tailoring the properties by defining the HHx content opens opportunities for a shift towards sustainable alternatives for a variety of conventional plastics as increasing the HHx content was shown to boost elasticity and improve processability due to lowered melting temperatures while maintaining remarkable tensile strength and biodegradability.

## CRediT authorship contribution statement

**Isabel Thiele:** Writing – review & editing, Writing – original draft, Visualization, Validation, Methodology, Investigation, Formal analysis, Data curation, Conceptualization. **Lara Santolin:** Writing – review & editing, Writing – original draft, Visualization, Validation, Methodology, Investigation, Formal analysis, Data curation, Conceptualization. **Klas Meyer:** Writing – review & editing, Writing – original draft, Visualization, Methodology, Investigation, Formal analysis, Data curation. **Rainhard Machatschek:** Writing – review & editing, Writing – original draft, Validation, Resources, Project administration, Methodology, Investigation, Funding acquisition, Formal analysis, Data curation. **Uwe Bölz:** Writing – review & editing, Writing – original draft, Data curation. **Natalia A. Tarazona:** Writing – review & editing, Writing – original draft, Visualization, Validation, Methodology, Investigation, Formal analysis, Data curation. **Sebastian L. Riedel:** Writing – review & editing, Writing – original draft, Validation, Supervision, Resources, Project administration, Methodology, Investigation, Funding

acquisition, Data curation, Conceptualization.

## Declaration of competing interest

The authors declare that they have no known competing financial interests or personal relationships that could have appeared to influence the work reported in this paper.

## Data availability

The data that support the findings of this study are available from the corresponding authors upon reasonable request.

## Acknowledgements

This research was supported by the German Federal Ministry of Education and Research, grant number 031B0833A and through the Helmholtz Foundation through Program Oriented Funding. We acknowledge support by the Open Access Publication Fund of BHT. Open Access funding enabled and organized by Projekt DEAL.

## Appendix A. Supplementary data

Supplementary data to this article can be found online at https://doi.org/10.1016/j.ijbiomac.2024.130188.

## References

[1] European Bioplastics, nova-Institute, Bioplastic Market Data [WWW Document], URL, https://www.european-bioplastics.org/market/, 2022.
[2] J.-G. Rosenboom, R. Langer, G. Traverso, Bioplastics for a circular economy, Nat. Rev. Mater. 7 (2) (2022) 117–137, https://doi.org/10.1038/s41578-021-00407-8.
[3] Y. Miyahara, A. Hiroe, S. Sato, T. Tsuge, S. Taguchi, Microbial Polyhydroxyalkanoates (PHAs): from synthetic biology to industrialization, in: Biopolymers for Biomedical and Biotechnological Applications, 2021, pp. 231–264, https://doi.org/10.1002/9783527818310.ch8.
[4] M. Erceg, T. Kovačić, I. Klarić, Thermal degradation of poly(3-hydroxybutyrate) plasticized with acetyl tributyl citrate, Polym. Degrad. Stab. 90 (2) (2005) 313–318, https://doi.org/10.1016/j.polymdegradstab. 2005.04.048.
[5] I. Chodák, R.S. Blackburn, 4 - sustainable synthetic fibres: the case of poly (hydroxyalkanoates) (PHA) and other fibres, in: R.S.B.T.-S.T. Blackburn (Ed.), Woodhead Publishing Series in Textiles, Woodhead Publishing, 2009, pp. 88–112, https://doi.org/10.1533/9781845696948.1.88.
[6] R. Turco, G. Santagata, I. Corrado, C. Pezzella, M. Di Serio, In vivo and post-synthesis strategies to enhance the properties of PHB-based materials: a review, Front. Bioeng. Biotechnol. 8 (2021) 619266, https://doi.org/10.3389/fbioe.2020.619266.
[7] I. Noda, P.R. Green, M.M. Satkowski, L.A. Schechtman, Preparation and properties of a novel class of polyhydroxyalkanoate copolymers, Biomacromolecules 6 (2) (2005) 580–586, https://doi.org/10.1021/bm049472m.
[8] C.F. Budde, S.L. Riedel, L.B. Willis, C. Rha, A.J. Sinskey, Production of poly(3-hydroxybutyrate-co-3-hydroxyhexanoate) from plant oil by engineered *Ralstonia eutropha* strains, Appl. Environ. Microbiol. 77 (9) (2011) 2847 LP–2854, https://doi.org/10.1128/AEM.02429-10.
[9] H. Arikawa, S. Sato, Impact of various β-ketothiolase genes on PHBHHx production in *Cupriavidus necator* H16 derivatives, Appl. Microbiol. Biotechnol. 106 (8) (2022) 3021–3032, https://doi.org/10.1007/s00253-022-11928-9.
[10] A.A. Kehail, M. Foshey, V. Chalivendra, C.J. Brigham, Thermal and mechanical characterization of solvent-cast poly(3-hydroxybutyrate-co-3-hydroxyhexanoate), J. Polym. Res. 22 (11) (2015) 216, https://doi.org/10.1007/s10965-015-0872-6.
[11] P. Murugan, C.-Y. Gan, K. Sudesh, Biosynthesis of P(3HB-*co*-3HHx) with improved molecular weights from a mixture of palm olein and fructose by *Cupriavidus necator* Re2058/pCB113, Int. J. Biol. Macromol. 102 (2017) 1112–1119, https://doi.org/10.1016/j.ijbiomac.2017.05.006.
[12] R.K. Purama, J.N. Al-Sabahi, K. Sudesh, Evaluation of date seed oil and date molasses as novel carbon sources for the production of poly(3Hydroxybutyrate-*co*-3Hydroxyhexanoate) by *Cupriavidus necator* H16 Re 2058/pCB113, Ind. Crop. Prod. 119 (2018) 83–92, https://doi.org/10.1016/j.indcrop.2018.04.013.
[13] L. Santolin, I. Thiele, P. Neubauer, S.L. Riedel, Tailoring the HHx monomer content of P(HB-*co*-HHx) by flexible substrate compositions: scale-up from deep-well-plates to laboratory bioreactor cultivations, Front. Bioeng. Biotechnol. 11 (2023) 1081072, https://doi.org/10.3389/fbioe.2023.1081072.
[14] R. Machatschek, B. Schulz, A. Lendlein, Langmuir monolayers as tools to study biodegradable polymer implant materials, Macromol. Rapid Commun. 40 (1) (2019) 1800611, https://doi.org/10.1002/marc.201800611.
[15] N.A. Tarazona, R. Machatschek, A. Lendlein, Unraveling the interplay between abiotic hydrolytic degradation and crystallization of bacterial polyesters comprising short and medium side-chain-length polyhydroxyalkanoates, Biomacromolecules 21 (2) (2020) 761–771, https://doi.org/10.1021/acs.biomac.9b01458.
[16] M. Bartels, B. Gutschmann, T. Widmer, T. Grimm, P. Neubauer, S.L. Riedel, Recovery of the PHA copolymer P(HB-co-HHx) with non-halogenated solvents: influences on molecular weight and HHx-content, Front. Bioeng. Biotechnol. 8 (2020) 944, https://doi.org/10.3389/fbioe.2020.00944.
[17] S. Hu, A.G. McDonald, E.R. Coats, Characterization of polyhydroxybutyrate biosynthesized from crude glycerol waste using mixed microbial consortia, J. Appl. Polym. Sci. 129 (3) (2013) 1314–1321, https://doi.org/10.1002/app.38820.
[18] F.M. Lamberti, L.A. Román, R. Joseph, Recycling of bioplastics: routes and benefits, J. Polym. Environ. 28 (10) (2020) 2551–2571, https://doi.org/10.1007/s10924-020-01795-8.
[19] R.M. Sivashankari, M. Mierzati, Y. Miyahara, S. Mizuno, C.T. Nomura, S. Taguchi, H. Abe, T. Tsuge, Exploring class I polyhydroxyalkanoate synthases with broad substrate specificity for polymerization of structurally diverse monomer units, Front. Bioeng. Biotechnol. 11 (2023) 1114946, https://doi.org/10.3389/fbioe.2023.1114946.
[20] Y.-M. Wong, C.J. Brigham, C. Rha, A.J. Sinskey, K. Sudesh, Biosynthesis and characterization of polyhydroxyalkanoate containing high 3-hydroxyhexanoate monomer fraction from crude palm kernel oil by recombinant *Cupriavidus necator*, Bioresour. Technol. 121 (2012) 320–327, https://doi.org/10.1016/j.biortech.2012.07.015.
[21] H. Mutlu, J.-F. Lutz, Reading polymers: sequencing of natural and synthetic macromolecules, Angew. Chem. Int. Ed. 53 (48) (2014) 13010–13019, https://doi.org/10.1002/anie.201406766.
[22] I. Noda, S.B. Lindsey, D. Caraway, in: G.G.-Q. Chen (Ed.), NodaxTM Class PHA Copolymers: Their Properties and Applications BT - Plastics from Bacteria: Natural Functions and Applications, Springer, Berlin Heidelberg, 2010, pp. 237–255, https://doi.org/10.1007/978-3-642-03287-5_10.
[23] Y. Doi, S. Kitamura, H. Abe, Microbial synthesis and characterization of poly(3-hydroxybutyrate-co-3-hydroxyhexanoate), Macromolecules 28 (14) (1995) 4822–4828, https://doi.org/10.1021/ma00118a007.
[24] S.L. Riedel, J. Bader, C.J. Brigham, C.F. Budde, Z.A.M. Yusof, C. Rha, A.J. Sinskey, Production of poly(3-hydroxybutyrate-*co*-3-hydroxyhexanoate) by *Ralstonia eutropha* in high cell density palm oil fermentations, Biotechnol. Bioeng. 109 (1) (2012) 74–83, https://doi.org/10.1002/bit.23283.
[25] Y. Feng, X. Jin, J.N. Hay, Evaluation of multiple melting peaks of propylene-ethylene copolymers, Polym. J. 30 (1998) 215–221.
[26] Y. Hu, J. Zhang, H. Sato, I. Noda, Y. Ozaki, Multiple melting behavior of poly(3-hydroxybutyrate-co-3-hydroxyhexanoate) investigated by differential scanning calorimetry and infrared spectroscopy, Polymer 48 (16) (2007) 4777–4785, https://doi.org/10.1016/j.polymer.2007.06.016.
[27] A. Werker, S. Bengtsson, P. Johansson, P. Magnusson, E. Gustaffson, M. Hjort, S. Anterrieu, L. Karabegovic, T. Alexandersson, A. Karlsson, F. Morgan-Sagastume, L. Sijstermans, M. Tietema, E. Wypkema, Y. Kooij, A. Deeke, C. Uijterlinde, L. Korving, Production Quality Control of Mixed Culture Poly(3-Hydroxbutyrate-co-3-Hydroxyvalerate) Blends Using Full-Scale Municipal Activated Sludge and Non-Chlorinated Solvent Extraction, 2021, p. 329.
[28] G. Tian, Q. Wu, S. Sun, I. Noda, G.-Q. Chen, Two-dimensional Fourier transform infrared spectroscopy study of biosynthesized poly(hydroxybutyrate-*co*-hydroxyhexanoate) and poly(hydroxybutyrate-co-hydroxyvalerate), J Polym Sci B 40 (7) (2002) 649–656, https://doi.org/10.1002/polb.10126.
[29] J. Asrar, H.E. Valentin, P.A. Berger, M. Tran, S.R. Padgette, J.R. Garbow, Biosynthesis and properties of poly(3-hydroxybutyrate-*co*-3-hydroxyhexanoate) polymers, Biomacromolecules 3 (5) (2002) 1006–1012, https://doi.org/10.1021/bm025543a.
[30] Q. Liao, I. Noda, C.W. Frank, Melt viscoelasticity of biodegradable poly(3-hydroxybutyrate-co-3-hydroxyhexanoate) copolymers, Polymer 50 (25) (2009) 6139–6148, https://doi.org/10.1016/j.polymer.2009.10.049.
[31] A. Jagoda, P. Ketikidis, M. Zinn, W. Meier, K. Kita-Tokarczyk, Interactions of biodegradable poly([R]-3-hydroxy-10-undecenoate) with 1,2-dioleoyl-sn-glycero-3-phosphocholine lipid: a monolayer study, Langmuir ACS J. Surf. Colloids 27 (17) (2011) 10878–10885, https://doi.org/10.1021/la201654d.
[32] Mohamed Isa bin Abd Majid, The Degradation of the phb and p (hb/hv) Copolymers and Their Uses in Drug Delivery, University of Bath, United Kingdom, 1988.
[33] S. Baidurah, P. Murugan, K.Y. Sen, Y. Furuyama, M. Nonome, K. Sudesh, Y. Ishida, Evaluation of soil burial biodegradation behavior of poly(3-hydroxybutyrate-*co*-3-hydroxyhexanoate) on the basis of change in copolymer composition monitored by thermally assisted hydrolysis and methylation-gas chromatography, J. Anal. Appl. Pyrolysis 137 (2019) 146–150, https://doi.org/10.1016/j.jaap.2018.11.020.
[34] A.P. Bonartsev, A.P. Boskhomodgiev, A.L. Iordanskii, G.A. Bonartseva, A. V. Rebrov, T.K. Makhina, V.L. Myshkina, S.A. Yakovlev, E.A. Filatova, E.A. Ivanov, D.V. Bagrov, G.E. Zaikov, Hydrolytic degradation of poly(3-hydroxybutyrate), polylactide and their derivatives: kinetics, crystallinity, and surface morphology, Mol. Cryst. Liq. Cryst. 556 (1) (2012) 288–300, https://doi.org/10.1080/15421406.2012.635982.
[35] Y.-W. Wang, W. Mo, H. Yao, Q. Wu, J. Chen, G.-Q. Chen, Biodegradation studies of poly(3-hydroxybutyrate-co-3-hydroxyhexanoate), Polym. Degrad. Stab. 85 (2) (2004) 815–821, https://doi.org/10.1016/j.polymdegradstab. 2004.02.010.
[36] J. Ravenstijn, Mimicking Nature - The PHA Industry Landscape. Latest Trends and 28 Producer Profiles, GO!PHA and nova-Institute, 2022, https://doi.org/10.52548/FUAQ6608.

[37] F. Masood, in: A.E. Oprea, A.M.B.T.-N.A. in F. Grumezescu (Eds.), Chapter 8 - Polyhydroxyalkanoates in the Food Packaging Industry, Academic Press, 2017, pp. 153–177, https://doi.org/10.1016/B978-0-12-811942-6.00008-X.
[38] L. Perez Amaro, H. Chen, A. Barghini, A. Corti, E. Chiellini, High performance compostable biocomposites based on bacterial polyesters suitable for injection molding and blow extrusion, Chem. Biochem. Eng. Q. 29 (2015) 261–274, https://doi.org/10.15255/CABEQ.2014.2259.
[39] D. Plackett, Biopolymers - new materials for sustainable films and coatings, in: Biopolymers - New Materials for Sustainable Films and Coatings, 2011, pp. 1–14, https://doi.org/10.1002/9781119994312.ch1.
[40] A.M. Díez-Pascual, A.L. Díez-Vicente, Poly(3-hydroxybutyrate)/ZnO bionanocomposites with improved mechanical, barrier and antibacterial properties, Int. J. Mol. Sci. 15 (6) (2014) 10950–10973, https://doi.org/10.3390/ijms150610950.
[41] F. Laoutid, H. Lenoir, A. Molins Santaeularia, A. Toncheva, T. Schouw, P. Dubois, Impact-resistant poly(3-hydroxybutyrate)/poly(ε-caprolactone)-based materials, through reactive melt processing, for compression-molding and 3D-printing applications, Materials 15 (22) (2022), https://doi.org/10.3390/ma15228233.
[42] H.J. Tang, S.Z. Neoh, K. Sudesh, A review on poly (3-hydroxybutyrate-co-[P(3HB-co-3HHx)]) and genetic modifications that affect its production, Front. Bioeng. Biotechnol. 10 (2022) 1057067, https://doi.org/10.3389/fbioe.2022.1057067.
[43] M.J. Fabra, G. Sánchez, A. López-Rubio, J.M. Lagaron, Microbiological and ageing performance of polyhydroxyalkanoate-based multilayer structures of interest in food packaging, LWT Food Sci. Technol. 59 (2, Part 1) (2014) 760–767, https://doi.org/10.1016/j.lwt.2014.07.021.
[44] A. Mukherjee, M. Koller, Microbial PolyHydroxyAlkanoate (PHA) biopolymers—intrinsically natural, Bioengineering 10 (7) (2023), https://doi.org/10.3390/bioengineering10070855.
[45] M. Bassas-Galià, A. Gonzalez, F. Micaux, V. Gaillard, U. Piantini, S. Schintke, M. Zinn, M. Mathieu, Chemical modification of polyhydroxyalkanoates (PHAs) for the preparation of hybrid biomaterials: FH - HES, CHIMIA 69 (2015), https://doi.org/10.2533/chimia.2015.627 (10 SE-Columns, Conference Reports), 627.
[46] M.S. Lehnertz, J.B. Mensah, R. Palkovits, Chemical recycling of polyhydroxybutyrate and polylactic acid over supported Ru catalysts, Green Chem. 24 (10) (2022) 3957–3963, https://doi.org/10.1039/D2GC00216G.
[47] S.A. Acharjee, P. Bharali, B. Gogoi, V. Sorhie, B. Walling, Alemtoshi., PHA-based bioplastic: a potential alternative to address microplastic pollution, Water Air Soil Pollut. 234 (1) (2023) 21, https://doi.org/10.1007/s11270-022-06029-2.
[48] B. Gutschmann, M. Maldonado Simões, T. Schiewe, E.S. Schröter, M. Münzberg, P. Neubauer, A. Bockisch, S.L. Riedel, Continuous feeding strategy for polyhydroxyalkanoate production from solid waste animal fat at laboratory- and pilot-scale, J. Microbial. Biotechnol. 16 (2) (2023) 295–306, https://doi.org/10.1111/1751-7915.14104.
[49] J. Ye, D. Hu, X. Che, X. Jiang, T. Li, J. Chen, H.M. Zhang, G.-Q. Chen, Engineering of Halomonas bluephagenesis for low cost production of poly(3-hydroxybutyrate-co-4-hydroxybutyrate) from glucose, Metab. Eng. 47 (2018) 143–152, https://doi.org/10.1016/j.ymben.2018.03.013.